Relation between Seismic Moment M_0 and Surface Wave Magnitude M_s

M. Rezapour[1,*] and R.G. Pearce[2]

[1]*Institute of Geophysics, Tehran University, Tehran, Islamic Republic of Iran*
[2]*Department of Geology and Geophysics, University of Edinburgh,*
West Mains Road, Edinburgh, EH9 3JW, U.K.

Abstract

The relation between M_S and $\log M_0$ is examined using Harvard CMT M_0, with both M_S^{Prague} and the improved surface wave magnitude scale M_S^t [1] applied to ISC data. Although M_S^t shows less scatter than M_S^{Prague}, neither dataset supports a slope of M_S against $\log M_0$ which tends to 1.0 towards smaller magnitudes. Instead, a good linear fit of slope 0.76 using M_S^t is found throughout the fitted range of M_0 (2.0×10^{24} to 1.26×10^{27} dyne-cm), and this linearity extends down to $M_0 = 2.5 \times 10^{23}$ dyne-cm. This suggests that previous proposals that M_S data support a theoretical slope of 1.0 in the low range of magnitude which may be expected from established relationships, is not justified.

Keywords: Magnitude; Surface wave; Seismic moment; ISC

Introduction

The objective of this article is to reassess the empirical relationship between surface-wave magnitude M_S and seismic moment M_0. This study was prompted by the introduction of a surface wave magnitude scale with improved distance correction (M_S^t) [1]. Magnitude, especially M_S, as a measure of earthquake strength, forms a basic dataset in seismology. However there is evidence of bias [2] in published M_0 as Central Moment Tensor (CMT) solutions, nowadays seismologists consider the seismic moment as a more reliable measure of earthquake size. Seismic moment is in theory a direct measure of earthquake size, whereas all magnitude scales are empirical. M_S is available for most significant earthquakes since about third decay of the twentieth century and some historical earthquakes, whereas routine estimates of M_0 by the Harvard group are only available since about 1977 for earthquakes having body-wave magnitude m_b of about 5 and greater. Therefore development of a reliable relationship between magnitude and seismic moment is of fundamental importance for integrating historical data into earthquake catalogues.

Most global agencies such as the International Seismological Centre (ISC) and the National Earthquake Information Center of the US geological survey (NEIC) routinely determine M_S using an empirical formula, the so-called "Prague formula" or "IASPEI formula" (International Association of Seismology and Physics of the Earth's Interior), given by

$$M_S^{\text{Prague}} = \log(\frac{A}{T})_{\max} + 1.66\log\Delta + 3.3, \qquad (1)$$

*E-mail: rezapour@ut.ac.ir

where A is half the peak-to-peak amplitude (on vertical component or resultant amplitude on two horizontal components) in microns, T is the wave period in seconds, and Δ is the epicentral distance in degrees [3]. Rezapour and Pearce [1] considered the theoretically-known contribution of dispersion and geometrical spreading, and introduced a modified M_S formula given by

$$M_s^t = \log(\frac{A}{T})_{max} + \frac{1}{3}\log \Delta$$
$$+ \frac{1}{2}\log(\sin \Delta) + 0.0046\,\Delta + 5.370, \tag{2}$$

They concluded that the M_s^t formula gives reduced bias for M_S in comparison with the Prague formula, and that there is less scatter in $\log M_0$ for a given M_0 when M_s^t is used. Ekström and Dziewonski [4], here referred to as ED88, presented evidence of systematic variations in M_S due to tectonic setting; they also fitted an analytical relationship to the M_S versus $\log M_0$ values.

In the CMT Catalogue the prime location information is that of the NEIC PDE (Preliminary Determination of Epicenters). Here the NEIC epicentral location and origin time (in the ISC Bulletin) were compared with those in the CMT Catalogue. Those epicentral estimates whose absolute values of differences are ≤ 0.2 degree in both latitude and longitude and absolute value of differences in origin times are ≤ 5 seconds are assumed to be the same earthquake. 6,553 earthquakes with available M_S and M_0 were selected in this way, for the time period from 1978 to 1993.

In this paper the relationship between seismic moment M_0 and two M_S scales, M_S^{Prague} (ISC) and M_s^t are compared using M_0 values obtained from the CMT Catalogue for the above dataset and the conclusions of ED88 are reexamined.

Analysis

Earliest studies have assumed a linear relation between surface-wave magnitude and the log of seismic moment. Under the hypothesis of constant stress drop, theoretical models predict that $\log M_0$ and M_S are indeed related linearly:

$$\log M_0 = A + BM_S, \tag{3}$$

The slope (B) commonly found in the literature [5-10] is around 1.5. However, the data and the range of magnitudes used by different authors were slightly different. An attempt to obtain a relation between

magnitude and seismic moment [7,11] resulted as:

$$M_S = \frac{2}{3}\log M_0 - 10.73, \tag{4}$$

where M_0 is seismic moment in dyne-cm. The relationship between seismic moment and earthquake energy is simplified by the observation that the stress drop is quite similar for virtually all earthquakes of magnitudes exceeding about 3. A constant stress drop in low-magnitude seismic data has been reported from a deep borehole [12]. For dataset containing smaller and large earthquakes, has been showed that earthquakes are self-similar over magnitude range $M \sim -2$ to ~ 8 [12]. Other seismologists for smaller earthquakes all from the same region reported that stress drop appears to increase with increasing moment for earthquakes below a critical size about 2.0×10^{20} dyne-cm, becoming constant for earthquakes larger than critical size [13].

The seismic moment represents the size of an earthquake only at a period much longer than the source process time (~source dimension / shear velocity), so it represent long-period end of the source spectrum [14]. For very large earthquake the corner frequency can fall below ~0.05 Hz (which used for M_S determination). In equation (4) because a theoretical slope of 1.0 is only predicted from instantaneous moment release on source rupturing surface, a different slope is to be expected for real data. Moreover, it has been argued [5,15] that the slope should decrease towards larger magnitude on account of the decreasing corner frequency, since the magnitude estimates are derived at a standard frequency.

ED88 chose to use a two-segment linear model, with a quadratic transition between the segments, to fit the global M_s versus $\log M_0$ data. They attempted to fit the averaged magnitude estimates for 2,341 earthquakes, to a hypothesized M_S:$\log M_0$ relation. In their analytical relation between M_S (as the dependent variable) and $\log M_0$ (as the independent variable) they imposed a slope of unity for small events, and $\frac{2}{3}$ for moderate to large events.

We use the above dataset of 6,553 earthquakes between 1978 and 1993. Magnitudes (M_S^{Prague} and M_s^t) have been recomputed from amplitude and period measurements in the ISC Catalogue to two decimal places, and corresponding M_0 values are taken from the CMT Catalogue. The individual data are plotted in Figures 1a and 1b for M_S^{Prague} and M_s^t respectively. The event magnitudes are averaged within each 0.1-wide interval of $\log M_0$ units, and are plotted in Figures 2a, and 2b.
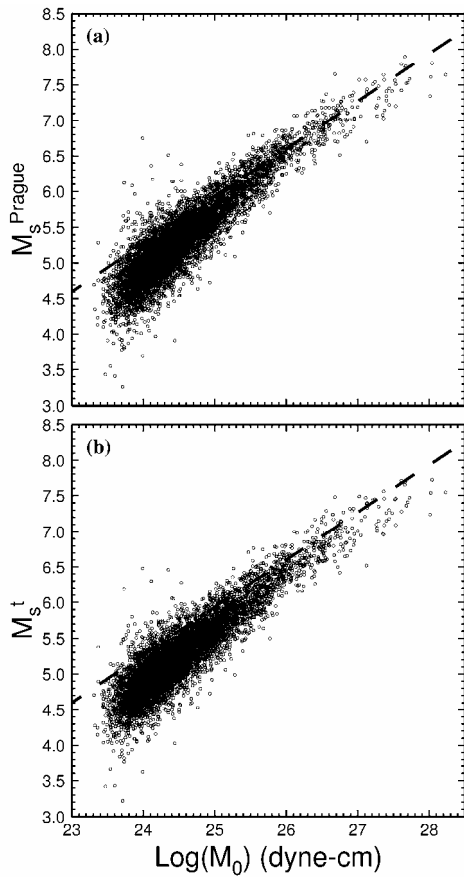
Figure 1. Distribution of M_s values against $\log M_0$ for individual data points 6,553. (a) for M_S^{Prague} values. (b) for M_S^t values. The relationship of Hanks and Kanamori [7] (our Equation 4) is shown by a thick dashed line in both graphs.

Figure 2. Average M_S values over 0.1-unit-wide intervals of $\log M_0$. (a) for M_S^{Prague} values. (b) for M_S^t values. In (a) and (b) the solid curve represents the ED88's analytical relation (their Eq. 2) and our Eq. (6) respectively, and the thin dashed line shows the linear regression fit to the same data. In (a) and (b) the thick dashed line shows the relationship of Hanks and Kanamori [7]. In (a) and (b) the range of data used in the fits is highlighted in gray.

There are some minor differences between this dataset (6,553 selected earthquakes) and that of ED88 resulting from their use of NEIC rather than ISC data. They used M_S^{NEIC} values from events for which both h^{NEIC} and h^{CMT} are less than 50 km, whereas here data from events with $h^{ISC} \leq 60$ km are used. Also, their data window was 1977-1987 whereas here 1978-1993 is used (consistent ISC M_S determination began in 1978). Although we use the same lower M_0 limit of 2.0×10^{24} dyne-cm for fitting, because of saturation a more restrictive upper limit of $M_0 = 1.26 \times 10^{27}$ dyne-cm is imposed, it seems the saturation in this dataset appears at this value. However, increasing the number of broad-band and very broad-band seismic stations all over world and using surface wave measurements from these station without the IASPEI restriction in period to M_S determination cases the saturation occurs at grater value.
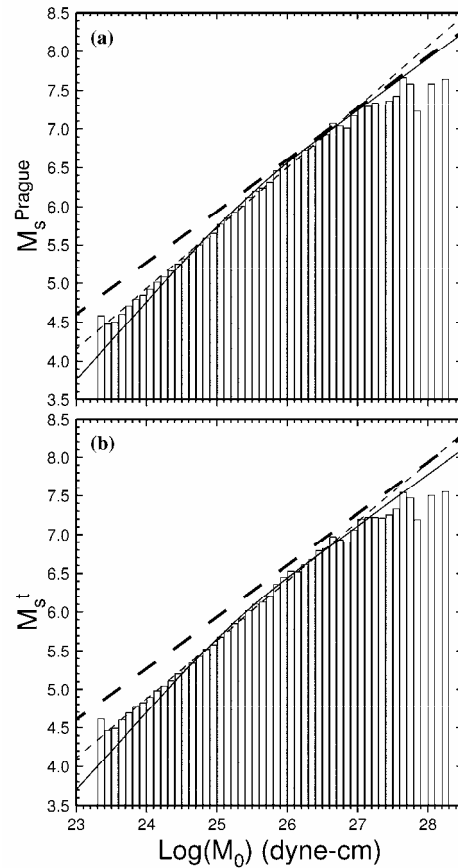
The analytic relation has three free parameters and is most easily represented using the formulation of ED88, except that we control the limits of the segments by constants A and B in units of M_0 (rather than $\log M_0$), in order to relate the constants to the graph more easily. We obtain

$$M_S = k - \frac{(\log A + \log B)}{6} + \log M_0 \quad \text{for } M_0 < A \quad (5a)$$

$$M_S = k - \frac{(\log A + \log B)}{6} + \log M_0$$

$$(5b)$$

$$- \frac{(\log M_0 - \log A)^2}{6(\log B - \log A)} \quad \text{for } A \leq M_0 \leq B$$

Table 1. Fitting parameters obtained when applying the analytical relation of Eqs. (5a, 5b, 5c) to the M_S^{Prague} and M_S^{t} datasets. a) Without a constraint of a segment with a slope of 1.0. b) Considering a minimum of two points are required to lie along a slope of 1.0. c) For applying a linear relation of $M_S = \alpha \log M_0 + \beta$

a) M_s formula	Parameters			Sum Squared Residuals (SSR)[a]				No. of data points[b]			
	k	A	B	$r1$	$r2$	$r3$	R	$n1$	$n2$	$n3$	N
M_s^{t}	-10.89	2.00×10^{24}	1.45×10^{26}	0.0000	0.0239	0.0275	0.0514	0	18	10	28
M_S^{Prague}	-10.78	2.00×10^{24}	2.57×10^{26}	0.0000	0.0158	0.0243	0.0401	0	21	7	28

b) M_s formula	Parameters			Sum Squared Residuals (SSR)				No. of data points			
	k	A	B	$r1$	$r2$	$r3$	R	$n1$	$n2$	$n3$	N
M_s^{t}	-10.89	2.88×10^{24}	1.29×10^{26}	0.0108	0.0179	0.0275	0.0563	2	16	10	28
M_S^{Prague}	-10.78	2.88×10^{24}	2.09×10^{26}	0.0047	0.0134	0.0245	0.0426	2	18	8	28

c) M_s formula	α	β	SSR	Correlation coefficient	N
M_s^{t}	0.763518 ± 0.011680	-13.448340 ± 0.300357	0.064944	0.996971	28
M_S^{Prague}	0.783727 ± 0.012359	-13.875954 ± 0.317816	0.072714	0.996783	28

[a] r1, r2, and r3, are respectively the Sum of the Squared Residuals of the three sections of the relationship in Eqs. (5a, 5b, 5c), and R is that for the total relation.
[b] n1, n2, n3, and N are the number of data points used to compute the four SSR values, respectively.

$$M_S = k + \frac{2}{3} \log M_0 \quad \text{for} \quad M_0 > B \qquad (5c)$$

We first attempt to fit an analytical function of the form proposed by ED88 using M_S^{t}. The results of our analysis are shown in Table 1. Table-1a shows the resulting fit when the Sum of the Squared Residuals (SSR) is minimized in k, A and B using M_S^{t} and the specified range of M_0. It is seen that A is equal to 2.0×10^{24} dyne-cm, which corresponds to the lower limit of the fitted range. Hence, no segment with a slope of 1.0 remains when the least-squares fit to the functions in Eqs. (5a,5b,5c) is optimized. The full relation is given by

$$M_S^{t} = -19.30 + \log M_0 \quad \text{for} \quad M_0 < 2.0 \times 10^{24} \quad (6a)$$

$$M_S^{t} = -19.30 + \log M_0 - 0.09(\log M_0 - 24.30)^2$$
$$\text{for} \quad 2.0 \times 10^{24} \leq M_0 \leq 1.45 \times 10^{26} \qquad (6b)$$

$$M_S^{t} = -10.89 + \frac{2}{3} \log M_0 \quad \text{for} \quad M_0 > 1.45 \times 10^{26} \quad (6c)$$

We next reassess the fit to Eqs. (5a,5b,5c) using M_S^{Prague} (Table-1a). Again we see that no segment of slope 1.0 remains, although the SSR is smaller than when M_S^{t} values are used.

The above results suggest that the observed data for M_S^{t} and even M_S^{Prague} do not provide evidence of a slope of unity for earthquakes in the relationship between M_s and $\log M_0$. If a minimum of two points are required to lie along a slope of 1.0 (Table-1b), then for M_S^{Prague} the values of k, A, and B are almost equivalent to those given by ED88.

The analytical relation of ED88 (their Eq. 2) and our fit (our Eqs. 6a, 6b, 6c) are plotted with solid curves, and the relationship of Hanks and Kanamori [7] is shown by a thick dashed line (Figs. 2a, 2b). Dark histogram bars are used to highlight the range of data used to compute the fit. These plots show visually that the evidence in support of the analytical relation proposed by ED88 is even weaker when the improved M_S^{t} scale is used. But by using a standard linear regression a better fit is obtained for M_S^{t} than for M_S^{Prague} as shown by thin dashed lines (Figs. 2b, 2a).

It is important to compare the success of testing different hypotheses. First, the sum squared residuals of fit in the both hypotheses using M_S^{t} scale are compared with residuals of fit using M_S^{Prague} scale. Comparison shows that the residuals in the case of applying analytical relation and using M_S^{t} values is larger than that for using M_S^{Prague} values, but this result is reverse in

the case of fitting a single linear regression (compare fitting parameters in Table-1b and Table-1c). For both M_S^{Prague} and M_s^t the residuals of fit is increased when a standard linear regression is applied. This is expected, because multiple linear and unlinear regressions analyze normally gives smaller residuals than only one single linear regression. The residuals of a single fit by using M_s^t values about 11% is reduced in comparison with using M_S^{Prague} values. Moreover, it is apparent (Figs. 2a, 2b) that a linear fit extends to smaller moments which were excluded from the fit because of possible incompleteness of earthquake catalogue, and also because of possible upward bias in M_s values close to the detection threshold. We use the same lower M_0 limit of 2.0×10^{24} dyne-cm for fitting as ED88 used. It is apparent that the goodness of fit strongly depends on the upper limit of fitted data, because the progressively smaller number of earthquakes towards higher moment create greater scatter, and because of the onset of magnitude saturation.

ED88's main reason for imposing a lower limit of 2.0×10^{24} dyne-cm when fitting their relation was the upward biasing of M_s Values caused by station threshold effects. Of course, this specific source of bias is governed by the bias in magnitude rather than moment. Figures 1a and 1b show a large scatter in the $\log M_0$: M_s: relation for individual events, particularly at smaller magnitude. If data points below, say $M_s=4.5$ are affected by station threshold bias, then this would have only a marginal effect on Figures 2a and 2b. We conclude that this source of bias does not contribute significantly to histograms with $\log M_0 > 23.4$ ($M_0 > 2.5 \times 10^{23}$ dyne-cm).

To examine the possible upward bias in low magnitude values we determined station correction (average $M_S^{event} - M_S^{station}$ values for each station) by using data of 10,894 earthquakes for which three or more observations have been used in the calculation of M_S^{ISC}. The average station correction in 0.1-unit-wide ranges of $\log M_0$ against $\log M_0$, and the histograms of used data are plotted respectively in Figures 3a and 3b for 6,553 earthquakes. Figure 3a shows that earthquakes with M_0 smaller than $\sim 10^{25}$ dyn-cm have been reported by individual stations in which most of station corrections ($M_S^{event} - M_S^{station}$) are positive. Therefore, by applying station correction, calculated M_S values will be increased about 0.1 for earthquakes with M_0 smaller than $\sim 10^{25}$ dyn-cm, this means the dataset used in this study does not show an upward bias in low magnitude values.

We conclude that data used here are more consistent with a linear fit than with the more complicated analytic relation of Eqs. (5a, 5b, 5c), and that this is so over the wider moment range from $M_0=2.5 \times 10^{23}$ to $M_0=1.26 \times 10^{27}$ dyne-cm, however in our analysis we used data range from 2.0×10^{24} to 1.26×10^{27} dyne-cm. This conclusion implies that $\log M_0$ is proportional to about $1.3 M_S$ over this wider magnitude range or M_S is proportional to $\log M_0$ as:

$$M_s^t = (0.763518 \pm 0.011680)\log M_0$$
$$- (13.448340 \pm 0.300357), \qquad (7)$$

The observed linear relationship suggests that the spectral fall-off above the corner frequency is not influencing M_s measurements at least up to $M_S \leq 7.2$. We can only speculate on the origin of the 0.76 gradient. We can be confident that it is not caused by inadequate distance correction since we are using M_S^t (Table 1c) although the difference between this value and the 0.78 obtained for M_S^{Prague} (Table 1c) may represent such an effect. One possibility is that the deviation of our gradient from 1.0 represents a dependence of stress drop $\Delta\sigma$ upon M_0. If this were so, a relation $\Delta\sigma \propto M_0^{0.14}$ is implied, which corresponds to a reduction in stress drop towards larger earthquakes.

The generation of 20-second surface-wave used in the M_S calculation depends on focal depth, focal mechanism as well as on the earth structure near the earthquake source or along the propagating path. In order to compare the focal mechanism effect on estimated M_S, the data are grouped. Here, following Frohlich and Apperson [17], earthquakes are grouped according to dip angle values of their P, B and T axes (δ_P, δ_B, and δ_T values) which were taken from Harvard source solutions. The mechanism is considered as strike-slip or normal faulting when dip angle of the B or P axes exceeds 60° respectively. When the T axis exceeds 50° the mechanism is proposed as thrust faulting. The M_S^t values for each group averaged over 0.1-unit-wide intervals of $\log M_0$ are plotted in Figure 4. This figure represents a set of (M_S^t, $\log M_0$) regression lines over a wide range of M_0 (2.5×10^{23} to 1.26×10^{27} dyne-cm) inferred from global distributed earthquakes with different focal mechanism. The values of the correlation coefficient, always greater than 0.97, indicate that the linear regression inversion is a good fitting. The thick solid (strike-slip) and gray (thrust) lines do not show much significant differences. The slope of thin solid line (normal earthquakes) is smaller

than of the other lines. Consequently, in the case of normal earthquakes, for a fixed value of $M_0 > \sim 10^{25}$, the magnitude M_S^t would be small (~ 0.1) in comparison with other earthquakes.

To compare average M_S^t in different tectonic settings defined as "oceanic ridges & fracture zones", "continental", and "subduction zones", the data were classified using Flinn-Engdahl seismic region number [16], and M_S^t values were averaged over 0.1-wide intervals of $\log M_0$. In Figure 5 average M_S versus $\log M_0$ are compared for different tectonic regions. This figure shows that the continental earthquakes have a larger M_S^t than corresponding earthquakes along mid-oceanic ridges and subduction zones with the same seismic moment. However, the largest earthquakes occur in subduction zones. For a given M_0 value, mid- oceanic ridge earthquakes have a smaller M_S^t than earthquakes in other regions. The difference between these regions is not constant and it increases with increasing seismic moment. Also, the number of individual data points controls the scatter of averaged data.
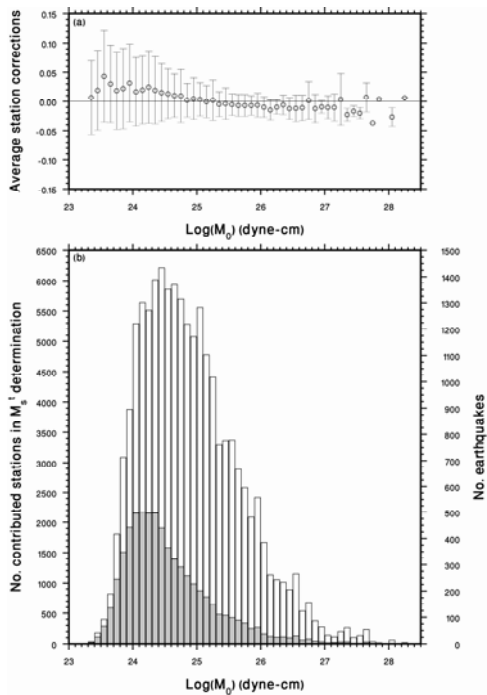
Conclusions

In the relation of M_S with $\log M_0$ the observed data do not provide evidence of a slope of unity towards smaller events when either the M_S^t or M_S^{Prague} scales are used. A simple linear regression gives a slope of 0.76 for M_S^t over a wide range of moments from 2.0×10^{24} to 1.26×10^{27} dyne-cm extending below the range used for fitting. The linear regression is less good for M_S^{Prague}. It is concluded that a linear fit of gradient 0.76 is preferable to the analytical relation of Eqs. (5a, 5b, 5c), making $\log M_0$ proportional to about $1.3 M_S$ over this wider moment range. Comparison of (M_S^t, $\log M_0$) relations for earthquakes with different focal mechanism do not show a very significant differences, but, the (M_S^t, $\log M_0$) relation for different tectonic settings shows a systematic bias.
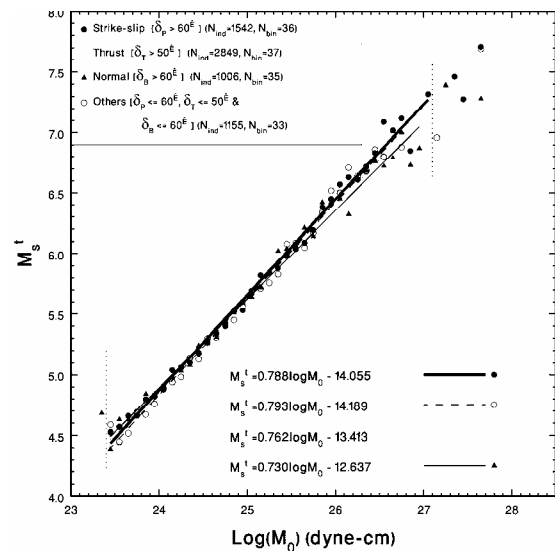

Figure 4. Average M_S^t over 0.1-wide intervals of $\log M_0$ against $\log M_0$ for earthquakes with different focal mechanism. Thick solid line, gray, and thin solid lines are the regression lines fitted to earthquakes with strike-slip, thrust and normal mechanism, respectively. The filled circles, squares, and triangles represent the average magnitude for earthquakes with strike-slip, thrust, and normal mechanism respectively. Open circles represent location of average data points for earthquakes in witch $\delta_P \leq 60°$, $\delta_T \leq 50°$, and $\delta_B \leq 60°$. The regression line for this group of earthquakes as earthquakes with other focal mechanism has been shown by dashed line. For regression analysis only the data points in the seismic moment range 2.5×10^{23} to 1.26×10^{27} dyne-cm were used which marked by vertical dotted lines. N_{ind} and N_{bin} represent the number of individual and the relevant binned data points, respectively.

Figure 3. (a) Average station corrections of 111,555 station records for 6,553 earthquakes over 0.1-wide intervals of $\log M_0$ against $\log M_0$. Error bars show a standard deviation of data points. (b) Histograms of dataset used in this study. White and gray histograms represent respectively number of contributed stations and earthquakes.
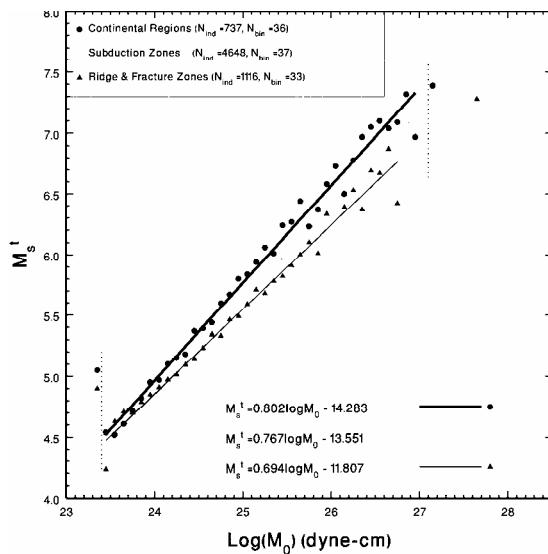
Figure 5. Average M_S^t over 0.1-wide intervals of $\log M_0$ against $\log M_0$ in different tectonic regions. The filled circles, squares and triangles represent the average magnitude for earthquakes in "continental", "subduction zones" and "oceanic ridges and fracture zones" respectively. The thick solid line, gray and thin solid lines represent linear regression lines to the data points in "continental", "subduction zones" and "oceanic ridges & fracture zones" respectively. For regression analysis only the data points in the seismic moment range 2.5×10^{23} to 1.26×10^{27} dyne-cm were used which marked by vertical dotted lines. N_{ind} and N_{bin} represent the number of individual and the relevant binned data points, respectively.

Acknowledgments

References

1. Rezapour M. and Pearce R.G. Bias in surface wave magnitude M_s due to inadequate distance corrections. *Bull. Seism. Soc. Am.*, **88**: 43-61 (1998).

2. Patton H.J. Bias in the centroid moment tensor for central Asian earthquakes: Evidence from regional surface wave data. *J. Geophys. Res.*, **103**: 26, 963-26, 974 (1998).

3. Vaněk J., Zatopek A., Karnik V., Kondorskaya N.V., Riznichenko Y.V., Savarensky E.F., Solov'ev S.L., and Shebalin N.V. Standardization of magnitude scales. *Bull. Acad. Sci. USSR, Geophys*, Ser. (English Transl.) No. 2, 108-111 (1962).

4. Ekström G. and Dziewonski A.D. Evidence of bias in estimations of earthquake size. *Nature*, **332**: 319-323 (1988).

5. Kanamori H. and Anderson D. Theoretical basis of some empirical relations in seismology. *Bull. Seism. Soc. Am.*, **65**: 1073-1095 (1975).

6. Purcaru G. and Berckhemer H. A magnitude scale for very large earthquakes. *Tectonophysics*, **49**: 189-198 (1978).

7. Hanks T.C. and Kanamori H. A moment magnitude scale. *J. Geophys. Res.*, **84**: 2348-2350 (1979).

8. Caputo M. and Console R. Statistical distribution of stress drops and faults of seismic regions, *Tectonophysics*, **67**: T13-T20 (1980).

9. Hyndman R.D. and Weichert D.H. Seismicity and rates of relative motion on the plate boundaries of Western North America. *Geophys. J. R. Astr. Soc.*, **72**: 59-82 (1983).

10. Dziewonski A.M. and Woodhouse J.H. An experiment in systematic study of global seismicity: Centroid-moment tensor solutions for 201 moderate and large earthquakes of 1981. *J. Geophys. Res.*, **88**: 3247-3271 (1983).

11. Kanamori H. The energy release in great earthquakes. *Ibid.*, **82**: 2981-2987 (1977).

12. Abercrombie R. and Leary P. Source parameters of small earthquakes recorded at 2.5 km depth, Cajon Pass, southern California: implications for earthquakes scaling. *Geophys. Res. Lett.*, **20**: 1511-1514 (1993).

13. Shi J., Kim W., and Richards P.G. The corner frequencies and stress drops of intraplate earthquakes in the northeastern United States. *Bull. Seism. Soc. Am.*, **88**: 531-542 (1998).

14. Kanamori H. Magnitude scale and quantification of earthquakes. *Tectonophysics*, **93**: 185-199 (1983).

15. Aki K. Scaling law of seismic spectrum. *J. Geophys. Res.* **72**: 1217-1231 (1967).

16. Flinn E.A., Engdahl E.R., and Hill A.R. Seismic and geographical regionalization. *Bull. Seism. Soc. Am.,* **64**: 771-993 (1974).

17. Frohlich C. and Apperson K.D. Earthquake focal mechanism, moment tensors, and the consistency of seismic activity near plate boundaries. *Tectonics*, **11**: 279-296 (1992).

18. Wessel P. and Smith W.H.F. New version of the Generic Mapping Tools released. EOS Trans. *Amer. Geophys., U.* **76**: 329 (1995).